

Cavities "Pit Number" and Micro-Jets Impingements

"Pit Number" de Cavidades e Ação de Micro-Jatos

Gil Bazanini¹; Nicodemus Neto da Costa Lima²; José Divo Bressan³

Abstract

Cavitation pits and erosion were obtained using the rotating disk device, where a steel disk with cavitation inducers and specimens fixed on it rotates inside a water chamber to provide the cavitating flow. These pits were observed with the aid of a scanning electronic microscopy. Micro-jets resulting from cavity collapse cause damages to solid surfaces. Because they are caused by the micro-jets, these pits are approximate circular. The exponent named pit number was calculated using the pit counting, that is the number of pits by area and by time unit. The influence of flow velocity was also analyzed here, and how greater is the flow velocity, how greater is the pit counting calculated. It was also calculated the distance from the collapsing cavity to the wall, considering a conic micro-jet.

Keywords: Cavitation. Pits. Erosion. Cavities. Micro-Jets.

Resumo

Foram obtidos erosão e "pits" de cavitação utilizando o dispositivo a disco rotativo, onde um disco contendo indutores de cavitação e os corpos de prova giram em uma câmara preenchida com água, visando causar escoamento cavitante. Estes "pits" puderam ser observados com auxílio de um microscópio eletrônico de varredura. Micro-jatos oriundos do desaparecimento da bolha, ou cavidade, causam danos à superfície sólida próxima. Pelo fato de serem causados por micro-jatos, os "pits" apresentam formato aproximadamente circular. O "pit number" foi calculado usando o "pit counting" que consiste no número de "pits" por unidade de área e de tempo. Observou-se ainda a influência da velocidade de escoamento no "pit counting": quanto maior a velocidade, maior o valor do "pit counting" calculado. Também foram calculadas as distâncias da cavidade até a parede, considerando micro-jatos cônicos.

Palavras-chave: Cavitação. "Pits". Erosão. Cavidades. Micro-Jatos.

¹ Dr. Prof., Depto de Engenharia Mecânica da UDESC, Joinville, SC, Brasil; E-mail: gil.bazanini@udesc.br

² Me. Prof., Depto de Engenharia Mecânica da UDESC, Joinville, SC, Brasil; E-mail: nicodemus.lima@udesc.br

³ Dr. Prof., Depto de Engenharia Mecânica da UDESC, Joinville, SC, Brasil; E-mail: josedivo.bressan@udesc.br

Introduction

The cavitation phenomenon, that is, the formation, growth and collapse of air and vapor cavities in liquids is, as well known, responsible for damage in metallic and non-metallic solid structures in liquid mediums, remarkably in water. Such cavities nucleate from micro-bubbles of air present in the liquid medium.

This cavity formation phenomenon is named "cavitation inception" (HAMMITT, 1980). The growth process involves primarily the action of pressure forces, but these are the result of the interplay of surface action, inertia and viscosity, and also gas diffusion and evaporation. In most simple terms, the conclusion results from the static force balance at the cavity wall between the surface tension and pressure differential:

$$P_V - P_L = \frac{2S}{R}, \quad (1)$$

where P signifies pressure at the cavity wall, the subscript v signifies vapor (and/or gas) and the subscript L signifies liquid. S is the surface tension, and R is the cavity radius.

As it grows, the cavity is filled by the liquid vapor, present when the pressure and temperature of the mixture are close to the vapor pressure and temperature of the surrounding liquid, until reaching an equilibrium radius as can be seen in Young (1989). After that, the cavity or cavities, begin their collapse and may disappear or initiate a new cycle, which may then be repeated for some times until the cavities disappear (YOUNG, 1989).

In the final stages of a cavity collapsing close to a solid wall, the cavity takes a toroidal form, from where the micro-jet emerges toward the wall (BAZANINI et al., 2017), impinging its surface.

With the goal to study the effects of cavitation on solid surfaces, several devices have been developed along the last decades, such as the cavitation test chamber (STELLER et al., 2005). Some of them are the jet-impact damage device (JANAKIRAM, 1973) that consists of water liquid jets impinging in specimens fixed on rotating disks, the vibratory apparatus (KNAPP et al., 1970) where the specimens are set to vibrate in the test liquid, the vertical (related to the axis) rotating disk (WOOD et al., 1967), where a disk with the specimens fixed on it is rotating in water to provide cavitating flow, and finally (the most important, because it reproduces the phenomenon of the flow through a pump) is the horizontal rotating disk device (ZHIYE, 1983; BAZANINI; BRESSAN, 2017).

There are several ways of analyzing the damage by cavitation: mass loss by erosion, area or volume loss as a function of time, and the "pit counting (PC)", or "pit

formation rate" (PFR), calculated by equation (2):

$$PC = \frac{Pits}{area \times time}. \quad (2)$$

The "pit formation rate" for metals can be expressed as an exponential function of the peripheral, considered as the flow velocity V , (ZHIYE, 1983) :

$$PFR \propto CV^n, \quad (3)$$

C and n (what is called "the pit number") are constants which depend on the material,

$$n = \frac{0.1}{UR}, \quad (4)$$

UR is the ultimate resilience of the material (kgf/mm²).

According to Zhiye (1983), n may be roughly estimated by:

$$n = \frac{0.51}{\sigma}, \quad (5)$$

where σ is the cavitation number:

$$\sigma = \frac{P_\infty - P_V}{\frac{1}{2}\rho_L V^2}, \quad (6)$$

ρ_L is the liquid density, P_∞ is the static pressure of the undisturbed liquid.

Experimental

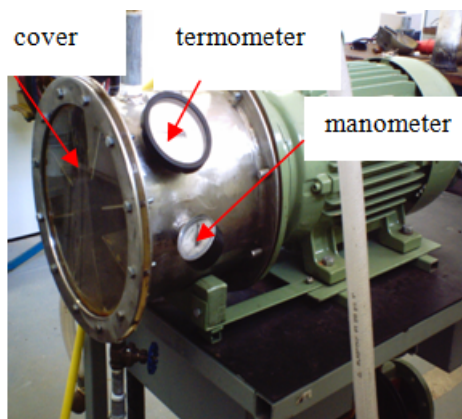
The device consists of a water chamber in which a metallic disk rotates. On the disk surface are located the cavity inducers, that are protruding pins, and the specimens as well. The disk is fixed on the shaft and may be detached to switch the specimens. A glass cover is mounted on the chamber to visualize the flow and the cavities formation inside.

The purpose of the device is to create the cavities that will be responsible for the damage of the specimens fixed on the disk surface and close to the inducers. To prevent vibration problems, the holes and the specimens are situated on opposite radial positions of their reciprocals. Vibration absorbers are also used at the equipment foundations, and the disk with the specimens were balanced before tests were performed. A side view of the rotating disk can be seen in figure 1 below.

Some authors, among them Zhiye (1983), used a cast iron chamber and protruding pins mounted on the disk. Here, the disk and the chamber are made by stainless steel, more resistant to cavitation erosion. It is being used the compact version of the device (BAZANINI; BRESSAN, 2017), that is, smaller chamber and disk diameter (250 mm), as well as a shorter shaft. By using the "Intermediary

Device", commonly used to connect pumps to electric motors, we can avoid the use of the bearing and the coupling, resulting in a shorter shaft. That is, the chamber now replaces the pump. This reduces loss transmissions as well as alignment problems.

Figure 1: Side view of the test rig.

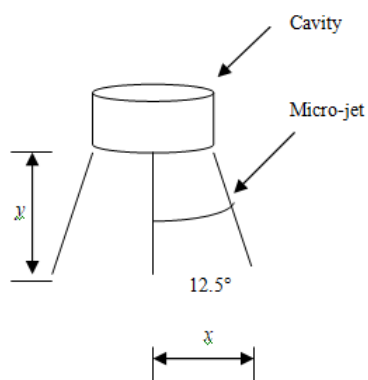


Source: The authors.

The Intermediary Device is made by cast bronze to prevent corrosion. Connections for inlet and outlet of water, temperature and pressure visualizations, and water drain and air outlet are also provided. Eight baffles equally spaced are welded in the chamber (and at a distance 18 mm from the disk) to kept cavities to collapse over the test specimens, avoiding pre-rotation of the test fluid (water). A frequency inverter is used to control the motor operation, and thus the disk rotation (BRESSAN et al., 2014).

According to Landau and Lifshitz (1987), based in experimental data, the water jet leaving a narrow vertical circular tube has a conical shape with an angle of 12.5 degrees to the vertical axis y (figure 2). Such hypothesis is considered here. An analogy is made here between the jet leaving a circular tube and a toroidal cavity.

Figure 2: Conic micro-jets from a toroidal cavity.



Source: The authors.

Where:

$$x = \frac{\phi_{pit}}{2} \quad (7)$$

and x is the half of the size of the cavitation pit, ϕ_{pit} measured in the images obtained from the experiments.

Considering a conic micro-jet, it is also possible to calculate the distance y from the collapsing cavity to the specimen.

The chemical composition of the test specimens used in the experiments are in Table 1.

Table 1: Chemical composition of the test specimens

Chemical element (% weight)	Aluminum
C	-
Pb	0.01
Zn	0.02
Al	98.24
Fe	0.22
Si	0.45
Cu	0.16
Mn	0.22
Mg	0.68

Source: BAZANINI, (2017)

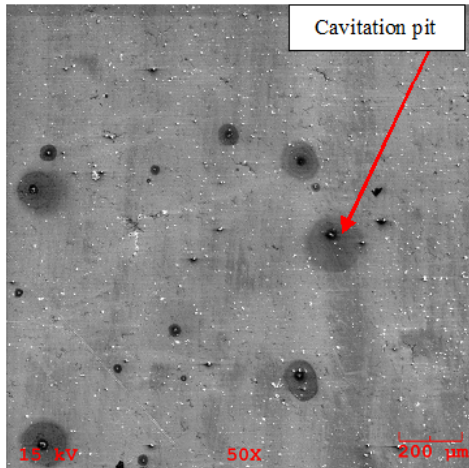
The "pit counting" was calculated for commercial aluminum by Bazanini (2017), based on the images from the scanning electronic microscope for the commercial aluminum using equation (2), for figure 3. Here, the exponent n will be calculated for the aluminum, using equations (3) to (5), working with data from this experiment as well as Saito and Sato's data (2003).

It was possible to detect the damages on the surface of the specimens after 5 and 10 hours in cavitating conditions for the commercial aluminum, using a scanning electronic microscope (BAZANINI, 2017). Some of these pits are seen in figures 3 and 4, after 5 and 10 hours, respectively (BAZANINI, 2017). They are similar to those obtained by Saito and Sato (2003). The pits are approximate circular in form, since they came from the micro-jets resulting from the final stages of collapse of air and vapor cavities, and they are approximate circular during almost all the process of collapse (BAZANINI et al., 2010).

Although it is not possible to see the shape of the micro-jets in the literature, the results of distances obtained here are close to the ones available in the bibliography, resulting in a good approximation for the micro-jets phenomena

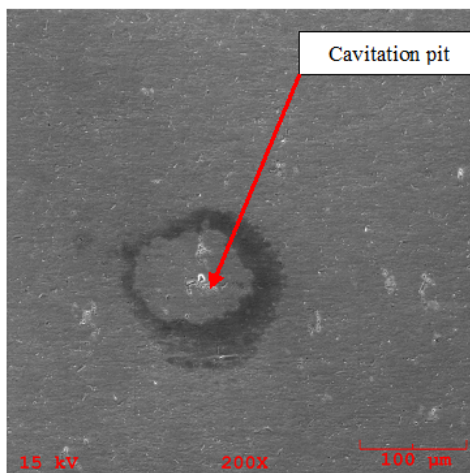
Using equation (2), the "pit counting" was calculated for each experiment and flow velocity (BAZANINI, 2017), for comparison purposes. It is noted that, for Saito and

Figure 3: Aluminum, 50x, after 5 hours.



Source: BAZANINI, (2017).

Figure 4: Aluminum, 200x, after 10 hours



Source: BAZANINI, (2017).

Sato (2003), the velocity of the flow in their test rig was remarkably smaller. For the aluminum (figure 3), the pits formed are very similar to the ones obtained by Saito and Sato (2003). They counted 10 pits in a circle of 3 mm in diameter, as listed in Table 2. In the present work, it was counted 15 pits in a square area of 1.5 x 1.5 mm, also in Table 2. The process of damages formation on the surface is usually a function of time. Saito and Sato (2003) experiments were performed during about 2 hours, while here the experiments took 5 hours in cavitation conditions, for the "pit counting".

Anyway, the "pit counting" calculations resulted 1.33 pits/(mm²xhour) in the present work, and 0.71 pits/(mm²xhour) for Saito and Sato (2003), who used a rig with a flow velocity of 3.6 m/s. Here, using the rotating disk device, it is attained greater values for the flow velocity, of 41.8 m/s, and the pit formation is also a function of the flow velocity (ZHIYE, 1983).

Table 2: "Pit counting" results

Author	Material	Flow velocity (m/s)	pits/(mm ² xhour)
SAITO; SATO, 2003	Al	3.6	0.71
BAZANINI, 2017	Al	41.8	1.33

Source: BAZANINI, (2017)

Results and Discussion

For the conical micro-jet and based on the images, the distances *y* of the collapsing cavities to the specimens were also calculated (Table 3). For figure 3, the pit used in the calculations is the indicated one, taken as an example. In the calculations, the cavity dimensions are being disregarded since it is in the final stage of collapse.

Table 3: Pits sizes and distances

Figure	3	4
$\phi_{pit}, \mu\text{m}$	178	120
$x, \mu\text{m}$	89	60
$y, \mu\text{m}$	401	271

Source: The authors.

According to Bressan et al. (2014), using equation (6), σ may vary from 0.077 to 0.098 when working with the rotating disk device. These will result for *n* the values of 6.6 to 5.2, respectively from equation (5).

Using the values of PC from Table 2 multiplied by the time of the experiments, it is possible to eliminate the time, such in the present work such as for Saito and Sato (2003) results. After that, by dividing one by the other we can eliminate the constant of proportionality as well as the constant *C*, resulting:

$$4.68 = 1.16^n, \tag{8}$$

from where $n = 10.4$.

Knapp et al. (1970) worked with aluminium leagues (1100, 2024 and 6061) to measure the weight loss by cavitation erosion. The *UR* of these leagues were used here to calculate *n* using equation (4).

Using the rotating disk device, (ZHIYE, 1983) attained a flow velocity of 43.2 m/s. Close to the one used in the present work. They worked with a value of 0.1115 for σ that was used in equation (5) here to calculate *n*.

The results obtained here for *n* from equations (3) to (5) are summarized in Table 4, using data of each author.

Table 4: Calculated n data for aluminum.

Equation	Authors	n
(3)	BAZANINI, 2017; SAITO; SATO, 2003	10,4
(4)	KNAPP et al., 1970	5.5 to 13.8
(4)	RAO et al., 1980	19.6
(5)	BRESSAN et al., 2014	5.2 to 6.6
(5)	ZHIYE, 1983	4.6

Source: The authors.

As one can see in the Table 4, from all calculations performed here, the calculated value of n varied from about 5 to 20.

Wood et al. (1967) used the rotating disk device with a flow velocity of 38.1 m/s working with alloys. They stated that the material volume loss is a function of the velocity flow as V^n where n varied from 1 to 10 for each alloy and damage condition.

All equations are meant to give approximate values only.

The distance from the cavity to the wall at the moment of the micro-jet may vary from 170 μm to 700 μm in images obtained by Tomita and Shima (1990). In the photographs from Hammitt (1980), it is possible to estimate roughly the distance from the cavity to the wall of about 200 μm . Such values are close to the ones obtained here.

Conclusions

The experiments worked quite well by creating cavitation damages on the surface of the metallic specimens.

Differences in the "pit counting" calculated based on the experiments made here and those from the literature are due to the differences on the time of the experiments as well as the flow velocities. That explains the greater values obtained here for the "pit counting", since we worked with greater values of flow velocities and our experiments took a longer time in cavitating conditions. Even though, the pits here are similar to those available in the literature which are very restrict, making impossible to make a better comparison.

Although it is not possible to visualize the shape of the micro-jets in the images from the literature, the conical model was reasonable good to explain the shape of the pits and the distances calculated, since those pits are approximate circular in shape. That does not mean that the shape will always be completely conical. Another possibility should be the hyperbolic micro-jets passing through the cavity, which is also symmetrical related to the y axis.

Equation (5) resulted in smaller values for n than equations (3) and (4) because it is based only in the characteristics of the flow, disregarding the mechanical properties of the material as well as the whole erosion process. Equations (3) and (4) are then more reliable to calculate the "pit number", giving results a little more close to each other when compared with equation (5).

Anyway, the distances calculated for the cavity to the wall is among experimental values available in the literature. The same applies to the exponent n , having in mind that all equations from the literature give just approximate values.

References

- BAZANINI, G., Cavitation Erosion Pits and Craters in Metals. *Semina: Ciências Exatas e Tecnológicas*, Londrina, v.38, p. 43-49, ago/dez 2017.
- BAZANINI, G.; BARBOSA JR., A. F.; LIMA, N. N. C. *Erosion and corrosion by micro-jets and high temperature cavity impaction on metal surfaces*. In: BRAZILIAN CONGRESS ON MANUFACTURING ENGINEERING, 9th, 2017, Joinville, Brazil, 2017.
- BAZANINI, G.; BRESSAN, J. D. Hot Vapor Bubble Prints on Carbon Steel. *Journal of Applied Mathematics and Physics*, Zürich, v. 5, p. 439-448, 2017.
- BAZANINI, G.; BRESSAN, J. D.; KLEMZ, M. A. Cavitation erosion of aluminum SAE-335 using the rotating disk device. *Revista SODEBRAS*, v. 5, n. 59, p. 10-13, nov. 2010.
- BRESSAN, J. D.; KLEMZ, M. A.; BAZANINI, G. *Cavitation erosion damage of metallic materials in rotating disk testing*. In: INTERNATIONAL BRAZILIAN CONFERENCE ON TRIBOLOGY, 2nd, 2014, Foz do Iguaçu, Brasil, Nov. 2014.
- HAMMITT, F. G. *Cavitation and multiphase flow phenomena*. New York: McGraw-Hill Book Company, 1980.
- JANAKIRAM, K. S. *Studies on erosion due to liquid jet impingement*. MSc. Thesis, Indian Institute of Science, Bangalore, June 1973.
- KNAPP, R. P.; DAILY, J. W.; HAMMITT, F. G. *Cavitation*. New York: McGraw-Hill., 1970.
- LANDAU, L. D.; LIFSHITZ, E. M. *Course of theoretical physics*. 2nd Edition. Great Britain: Pergamon Press, 1987. v. 6. Fluid mechanics.

RAO, P. V.; RAO, B. C. S.; RAO; N. S. L. Erosion and cavity characteristics in rotating components. *Journal of Testing and Evaluation*, Philadelphia, v. 8, p. 127-142, 1980.

SAITO, S.; SATO, K. *Cavitation bubble collapse and impact in the wake of a circular cylinder*. In: INTERNATIONAL SYMPOSIUM ON CAVITATION, 5th, Osaka, Japan, Nov. 2003.

STELLER, J.; KRELLA, A.; KORONOWICS, J.; JANICKILI, W. *Towards quantitative assessment of material resistance to cavitation, erosion*. *Wear*, 258, p. 604-613, 2005.

TOMITA, Y.; SHIMA, A. High-speed photographic observations of laser-induced cavitation, bubbles in water. *Acustica*, v. 71, n. 3, p. 161-171, 1990.

WOOD, G. M.; KNUDSEN, L. K.; HAMMITT, F. G. Cavitation Damage Studies with Rotating Disk in Water. Transactions of the ASME. *Journal of Basic Engineering*, New York, US, v. 89, p. 98-110, 1967.

YOUNG, F. R. Cavitation. New York: McGraw-Hill Book Company, 1989.

ZHIYE, J. *An experimental investigation on cavitation erosion for propeller alloys*. China: China Ship Scientific Research Center Report, 1983.

Received: Oct. 16, 2018
Accepted: Dec. 3, 2018